Soils and Rocks
An International Journal of Geotechnical and Geoenvironmental Engineering
www.soilsandrocks.com
ISSN 1980-9743
ISSN-e 2675-5475

Measuring deformation processes in granular materials from intragranular to bulk scales

Stephen Alexander Hall[1#]

Review Article

Keywords
Granular mechanics
Full-field measurements
Micro-structure
Micro-mechanics
X-ray tomography
X-ray diffraction

Abstract

Granular materials (assemblies of contacting grains with inter-granular porosity) form a vast family of materials important in both natural and industrial contexts. Under mechanical loads such systems show complex behaviours relating to the inter- and intra-granular stresses, strains and force transmission as well as the individual grain kinematics and interactions leading to multi-scale, heterogeneous behaviour. To understand such systems requires detailed understanding of these different structures and processes at the pertinent scales. This paper provides a brief overview of some new opportunities for enhanced experimental description of structures and mechanisms relating to the deformation of granular materials exploiting the penetrating power of x-rays for both imaging, giving access to granular structures and their evolution, and diffraction-based measurements, giving access to intra-granular grain structure and changes as well as inter- and intra-granular force transmission.

1. Introduction

Granular materials (assemblies of contacting grains with inter-granular porosity) form a vast family of materials important in both natural and industrial contexts, e.g., slope stability, avalanches, pharmaceutical tablet compaction, building foundations, powder-based additive manufacturing and food processing, to name but a few. Such materials are highly complex and can behave as liquids, gases or load-bearing solids, depending on their confinement, such that granular media are often considered to be another state of matter (e.g., Jaeger et al., 1996). The complex behaviour of these granular systems stems from the mobility and collective interactions of relatively simple building blocks (i.e., contacting particles) that together produce the bulk material behaviours and structural evolution. The processes controlling the bulk behaviours originate in mechanisms over a range of spatial and temporal scales from intra-granular mechanisms to contacting-particle interactions, intermediate (meso-) scale correlations and structure formation (e.g., localised deformation such as shear bands) to long-range pattern formation. These kinematic effects are associated with the build-up of stress, within grains and across granular structures, and relaxation via structural reorganisation and particle damage or breakage.

Granular mechanics have been studied for centuries, starting perhaps with the work of Coulomb in the late 1700s, but there remain key pieces of information regarding the (micro)mechanics that have been challenging to characterise. In particular, the measurement and understanding of force transfer and stress heterogeneity has, until recently, been missing in experimental studies. Furthermore, the role and evolution of heterogeneity at different scales is generally not captured in experiments and is, thus, often neglected in modelling. Therefore, more detailed experimental investigations and new techniques with a focus on capturing the necessary details for more accurate simulation models are required. Recent experimental developments are yielding new data and new understanding on heterogeneity, kinematics and force transfer from intra-granular and grain-grain contact scales to the granular-system scale that should provide improved support for advances in theoretical and numerical modelling of granular systems.

On the flip side to the experimental understanding, ever more sophisticated and detailed models and numerical simulation approaches are being proposed that aim to capture the complexities of granular micro-mechanics. These models can involve explicit representations of the granular frame, e.g., Discrete Element Method type approaches, or continuum models with constitutive laws based on phenomenological or micromechanics representations of the granular structure and evolution implemented in, for example, a finite element framework. However, in the words of Richard P. Feynman, "*It doesn't matter how beautiful your theory is, it doesn't matter how smart you are. If it doesn't agree with experiment, it's wrong*". More precisely (for granular mechanics), if the appropriate experimental data do not exist then a theory cannot be fully developed or validated, i.e., higher-order modelling requires equivalent higher-order experimental data for parameterisation, calibration and validation, as

#Corresponding author. E-mail address: stephen.hall@solid.lth.se
[1]Division of Solid Mechanics, Lund University, Lund, Sweden.

Submitted on May 30, 2024; Final Acceptance on June 19, 2024; Discussion open until November 30, 2024.
https://doi.org/10.28927/SR.2024.004324

well as to identify the mechanisms and phenomena that models should include (or not) for accurate representation of material responses.

This paper provides a brief overview of some new opportunities for enhanced experimental description of structures and mechanisms relating to the deformation of granular materials motivated by the need for ever more accurate modelling capabilities. The experimental approaches described exploit the penetrating power of x-rays for both imaging, giving access to granular structures, and diffraction-based measurements, giving access to the intra-granular crystalline grain structure and changes. It is noted that this is not a thorough review of the field, rather an overview of recent developments in which the author has been involved.

2. Full-field imaging of deformation, granular structure and structural evolution

It is well understood that mechanical loading of granular systems leads to localised deformation, consequently standard experimental approaches that capture just limited measurements (e.g., axial force, piston displacement, confining pressure, pore pressure) at a sample boundary can only provide a partial understanding of the processes occurring during the deformation. Localisation implies heterogeneity, which can also exist due to sample preparation or natural structure. Measurements at the sample boundary can only be interpreted with an assumption of homogeneity and be considered as some form of sample-averaged response. Such measurements can be used to calibrate/validate material models, if the full sample is modelled (e.g., with a finite or discrete element simulation), including the correct boundary conditions, but there will be ambiguity in this and little constraint on the evolving heterogeneity in structure and deformation. There can also be ambiguity as to the actual boundary conditions applied, as opposed to those that were envisaged, e.g., due to the contact of the sample with the loading pistons. Full-field measurements (e.g., Viggiani & Hall, 2012) aim to provide a field of measurements over a whole sample, which, when combined with "in-situ" imaging (i.e., imaging during the experiment with the sample set-up in-situ in the imaging system) can be used to track the evolution of the material and assess the actual boundary conditions experienced by the sample.

One of the most powerful tools for full-field imaging with in-situ experiments is x-ray (micro) tomography. Already in the 1960s x-rays were being exploited in geomechanics to follow internal deformation mechanisms in soil testing. This was mostly with radiography of 2D experiments, but some developments towards 3D were reported (e.g., Arthur & Dunstan, 1969). These works revealed, for example, dilation associated with shear localisation in granular media (e.g., Stone, 1985). In the 1980s, Desrues et al. (1996), utilised medical x-ray tomography to reveal the internal structural evolution of shear bands in triaxial tests on sand (e.g., Desrues et al., 1996). Importantly, in this work, in addition to characterising the 3D structure of the strain localisation, quantitative information was extracted from the images to reveal details about the material behaviour, such as the local evolution of void ratio and the local applicability of critical state theory. The past 20 years have seen significant developments in the x-ray tomography technique as well as in its accessibility and utilisation. In particular, laboratory x-ray microtomographs are now present in many labs around the world enabling micron to 10s-micron resolution 3D imaging of samples, including during experiments performed inside an imaging device (called herein in-situ experiments). As such, the experiments of Desrues et al. (1996) were repeated in recent years to reveal even finer details of the strain localisation evolution, including through quantified measurements of the strain field by Digital Volume Correlation (DVC) (discussed below) (Desrues et al., 2018).

An alternative to laboratory x-ray microtomography is to use a synchrotron facility, such as the European Synchrotron X-ray Facility (ESRF) in Grenoble, France. Such facilities provide higher-speed, higher resolution imaging for more detailed studies of evolving deformation. Early work using synchrotron tomography in granular mechanics includes that of Hall et al. (2010a), in which a triaxial compression experiment was performed in-situ in the synchrotron imaging station (beamline ID15 at the ESRF). Figure 1 shows images from the experimental set-up as well as the sample stress-strain response and a 3D rendering of the x-ray tomography image in the initial state. A general limitation of synchrotron imaging is the field-of-view (FoV) that is possible, although this is becoming less of a constraint with the development of the facilities and the techniques. Furthermore, the spatial resolution is generally linked to the FoV: the higher the resolution required, the smaller the FoV. Consequently, synchrotron imaging is generally performed on reduced sized samples, compared to standard laboratory testing. In the case of Hall et al. (2010a, b), the sample size was 22 mm high and 11 mm in diameter, but this enabled a voxel size (a voxel is a 3D pixel) of 14×14×14 μm^3 giving about 20 voxels across a grain diameter. From such images, it is possible to separate the grains from the pore space and to distinguish individual grains. Consequently, through 3D image analysis techniques, porosity fields can be derived as well as measurements on all the grains in the sample (in this case about 50 000 grains), such as their size and shape, plus the contacts between grains can be identified and quantified, e.g., in terms of orientation distribution (fabric) (see Figure 2).

In-situ experiments, such as those described above, involve loading the specimen inside the imaging set-up, which enables 3D images to be acquired through the loading. This provides 4D data sets (3D + time) enabling the evolution of the measurements, such as those highlighted in Figure 2, to be tracked through the experiment. Therefore, porosity or contact evolution can, for example, be monitored in a full-field sense.

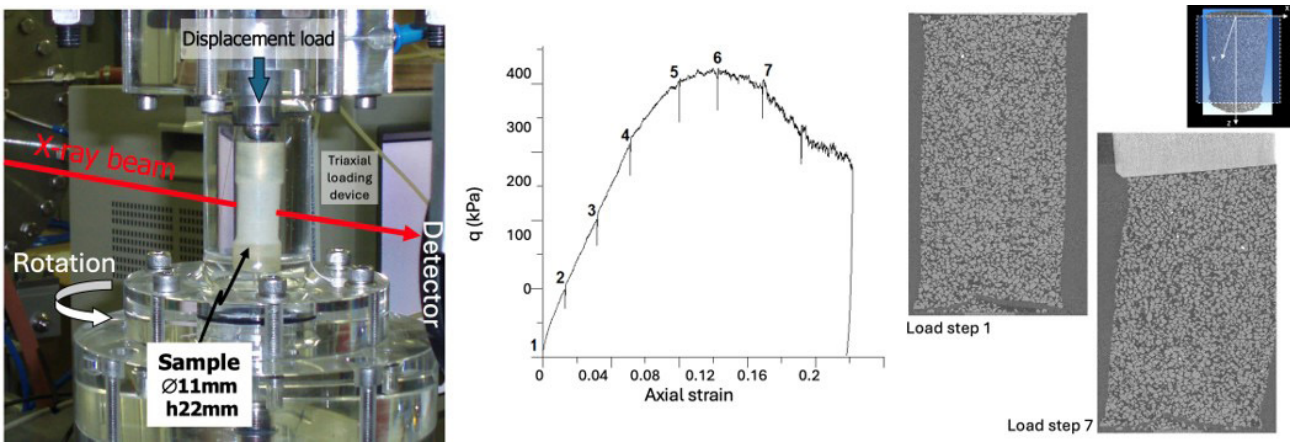

Figure 1. Left: Mini-triaxial compression experimental set-up of Hall et al. (2010a) at the ID19 beamline of ESRF. Middle: deviatoric stress (q) versus axial strain curve with imaging points indicated by numbers (the stress drops are due to stopping of the piston displacement during the imaging). Right: slices through the 3D x-ray tomography volumes acquired at the start of deviatoric loading and at load step 7 (plus inset showing the slice plane through the volume).

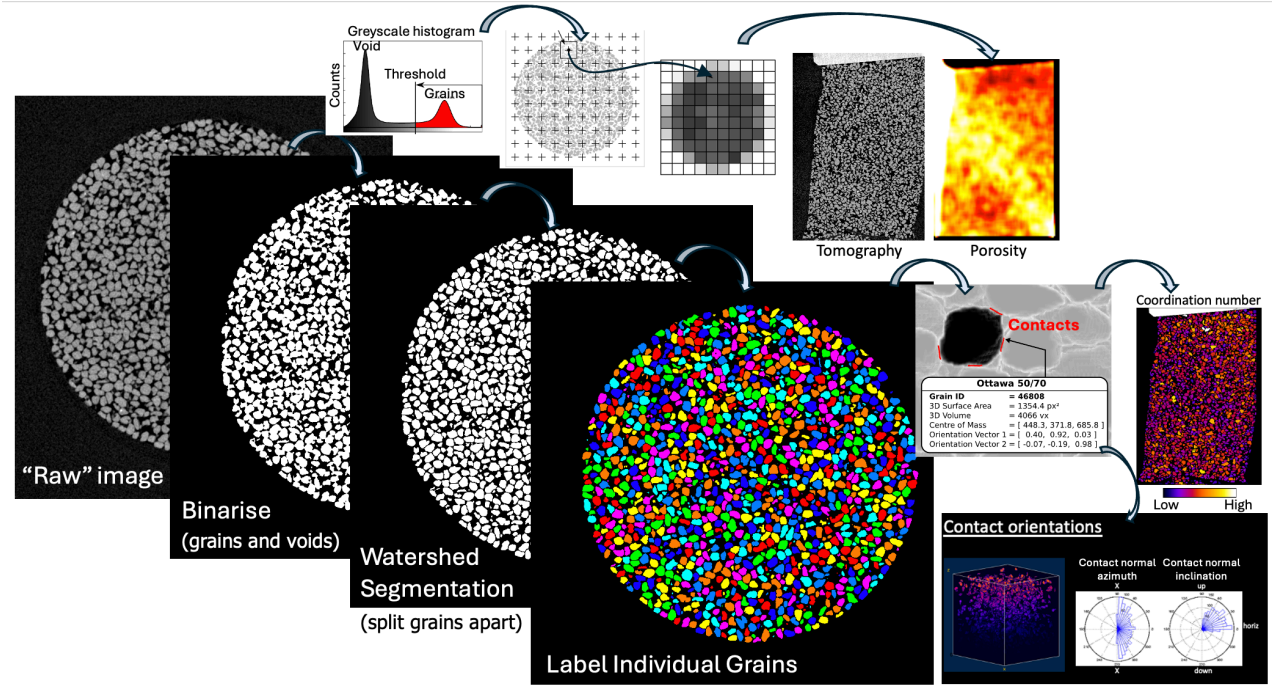

Figure 2. Schematic of the 3D image quantification process indicating how the "raw" greyscale 3D x-ray tomography images can be binarized by a simple thresholding approach to be used directly to calculate porosity fields by concatenation of the black:white voxel count over small image subsets or to separate the individual grains (e.g., by a watershed algorithm) to enable quantification of the individual grain characteristics, and contacts (images adapted from Andò, 2013; Andò et al., 2012; Hall et al., 2010a).

Furthermore, DVC can be used to follow parts of the image from one step to the next to derive 3D vector displacement fields from which, by differentiation, 3D tensor strain fields can be derived (Figure 3) (see, for example, Hall et al., 2010a; Hall, 2012). The standard DVC approach considers the image simply as a set of voxels with different intensities, ignoring any microstructure. An alternative approach to DVC is to respect the microstructural information contained in the images and, for the case of granular materials, track the individual grains instead of just cubic subsets of the image (see Figure 4). This approach requires a segmented image volume where all the grains are individually labelled. The outputs from such "discrete DVC" (D-DVC) are the full kinematics of every grain in the sample through the loading experiment (e.g.,

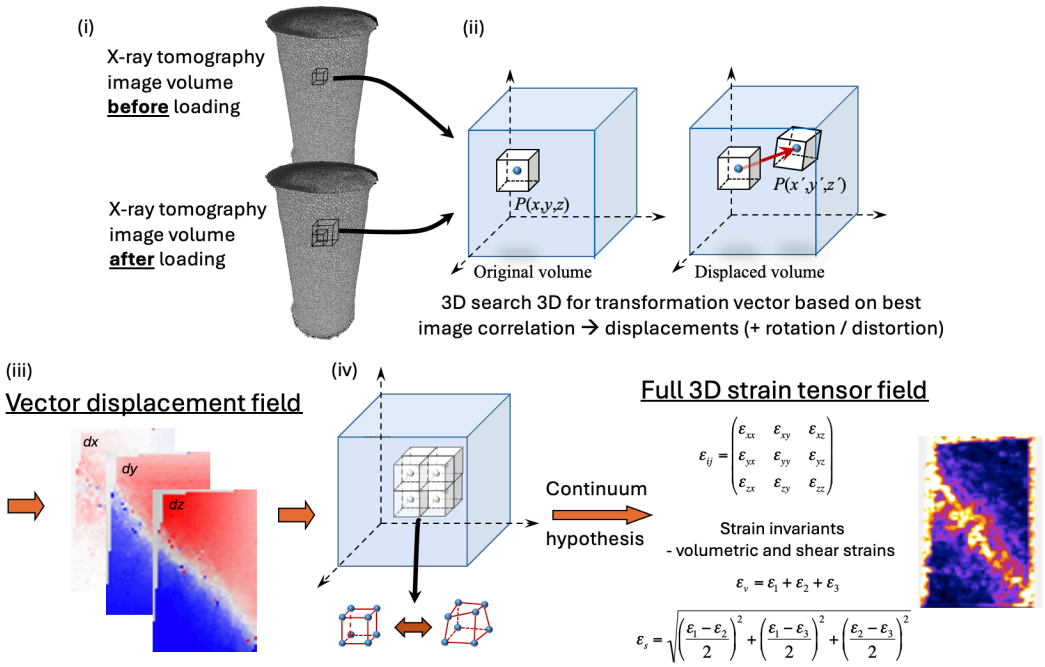

Figure 3. Schematic of a DVC involving: (i) defining a 3D grid of analysis points (nodes) in the initial 3D x-ray tomography volume; (ii) small image volumes are extracted from around each node; (iii) displacements of each node from the first image to the next is determined by a search for the translations (plus eventually rotations and deformations) that give the best correlation to equivalent volumes in the second image (usually derived with sub-pixel resolution); (iv) the resulting 3D vector field of nodal displacements (indicated by the 3 slices through the *dx*, *dy*, *dz* volumes) can be used to define, by differentiation, the 3D tensor strain field that is often represented in terms of strain invariant scalars, as in the slice through the shear strain field volume shown.

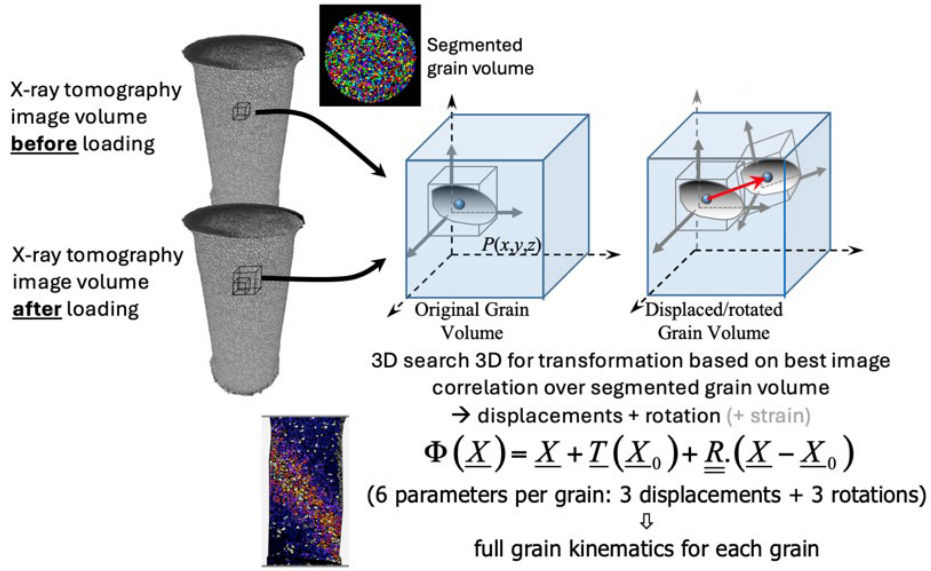

Figure 4. Schematic of a D-DVC approach, utilises the segmented grain map (see Figure 2) to define the grain centres and a mask to isolate the grain voxels in a small volume around the grain centre. A correlation search is performed, in a similar way to standard DVC (Fig. 3), refining for displacement and rotation with an assumption (usually) of incompressible grains (although grain strain can be assessed in the SPAM implementation (Stamati et al., 2020)). The output is a set of 3-component displacement vectors and 3-component rotation vectors for all the grains in the assembly. Continuum strain fields can be derived by tessellation of the grain centres and differentiation of the grain displacements.

Hall et al., 2010a). Put together, the in-situ experiments with x-ray tomography and 3D/4D image analysis can provide a quite complete picture of granular evolution during triaxial experiments, as indicated in Figure 5.

Building on the work of Hall et al. (2010a, b), Andò (2013) produced significant developments to the above-described granular experimental micromechanics approach including running similar, grain-resolution experiments with a laboratory tomograph, acquiring many more images per test (10s), comparing different grain types and advancing the image analysis algorithms. Furthermore, the SPAM software for DVC has subsequently been developed with specific adaptations for the analysis of granular materials, including D-DVC for grain tracking (Stamati et al., 2020). The experimental and image analysis advances, including the development of SPAM, have promoted a better understanding of the micromechanics of granular materials (e.g., Andò et al., 2012; Andò et al., 2013; Wiebicke et al., 2020; Zhao et al., 2021; Pinzón et al., 2023).

3. Grain scale imaging of granular deformation, granular stress/strain and force transfer

Whilst the experimental and analysis approaches with in-situ x-ray tomography described above have provided rich, previously inaccessible details on granular deformation mechanisms, they remain limited to measurements of structure and kinematic quantities. Mechanical analysis, however, must also consider the transfer of forces and stress in the system for a complete picture. As with kinematic measurements, forces are generally only measurable at the boundary of a specimen and only some components of the stress can be evaluated, even in the advanced approaches described above. Furthermore, as with kinematic measurements, standard measurements do not give a complete picture of the actual boundary conditions and stress conditions experienced by the sample, e.g., due to limited measurement possibilities and friction effects. To address this challenge, the use of x-ray (and neutron) diffraction approaches has been proposed (e.g., Hall et al., 2011) to measure the crystallographic (elastic) deformation of the constituent grains in a granular sample, which can be interpreted in term of stress through Hooke's law.

X-ray diffraction occurs through coherent elastic scattering of x-rays from the electrons surrounding atoms. The well organised distribution of atoms in crystal structures leads to constructive interference of the scattered x-rays to give, so-called, diffraction peaks at well-defined scattering angles. This phenomenon can be described by Bragg's law where the diffraction angle, 2θ, between the incoming x-rays and the outgoing diffracted x-rays is related to the x-ray wavelength, λ, and the crystallographic spacing, d_{hkl}, of each

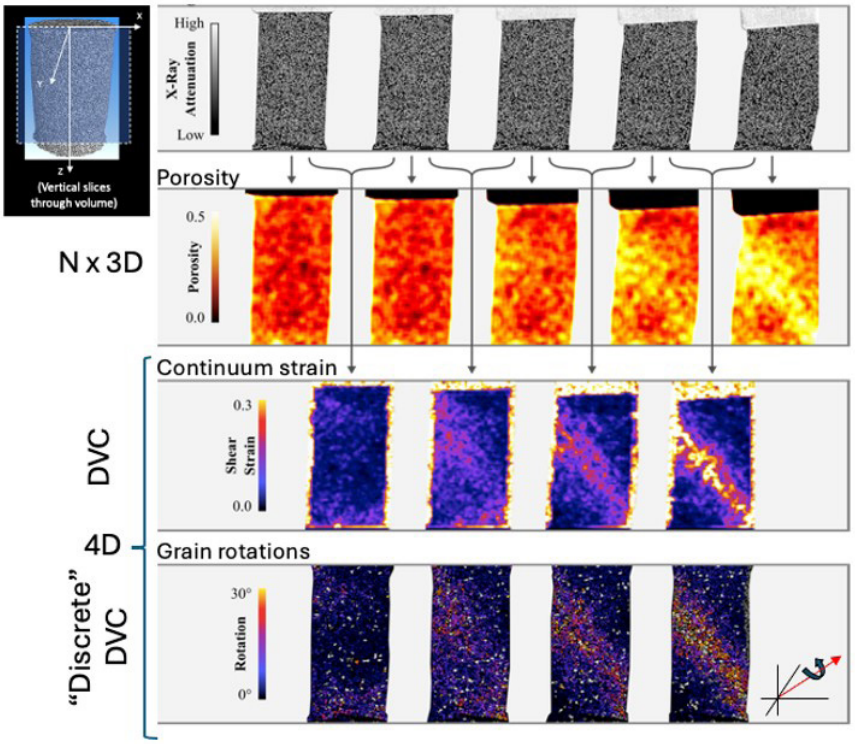

Figure 5. Example of the possible outputs from 3D and 4D image analysis of x-ray tomography data (top row) in terms of porosity field mapping, DVC-derived strains and grain kinematics from D-DVC. All analysis is in 3D but slices through the volumes are shown presenting representative components of the vector or tensor fields. (images adapted from Hall et al., 2012).

specific set of crystallographic planes in a crystal described by the Miller indices, *h, k, l*. For the case of single crystals, a few well-defined diffraction peaks can be measured in different directions relative to the incoming beam and sample orientation. Rotation of the sample can provide a set of peak measurements that can be interpreted to give the crystal orientation and the spacing of the crystallographic planes. In the case of a polycrystalline material consisting of many individual crystal grains, additional analysis is required to separate the signals from each grain; this is known as 3DXRD as described by, e.g., Poulsen (2008). For the case where the x-ray beam illuminates the full sample (e.g., Figure 6) this can be referred to as full-field 3DXRD (ff3DXRD). 3DXRD was first developed for metal samples but has also been applied to granular materials consisting of crystalline grains, as first demonstrated by Hall et al. (2011).

Figure 6 indicates a combined ff3DXRD and x-ray tomography workflow for granular mechanics studies. The sample is fully illuminated by a broad x-ray beam, which could involve full illumination of the sample diameter, and, with stitching, several vertically offset measurements can be used to cover the sample height. Rotation of the sample around the vertical axis provides a set of 2D diffraction patterns that can be analysed (e.g., by imageD11; Wright, 2020), to yield the individual diffraction patterns for each grain. This allows the evaluation of the grains' centres of mass, crystallographic orientations, and unit cell parameters (which describe the crystallographic structure such as the lattice spacings). Repeating such measurements at different stages of loading can, thus, provide measurements of grain rotations (from the orientation change - usually at higher resolution than possible from tomography images) and grain-averaged strain tensors (from the changes in the unit cell parameters), as well as continuum strain fields through tessellation of the grain centre positions and their displacements. Figure 7 shows example results from Hall & Wright (2015) on the evolution of the granular strains as a function of loading for a small assembly of single crystal quartz grains showing the evolution of the strain tensors for different grains and 3D renderings of the strain tensors on the grains shapes derived from x-ray tomography images of the sample acquired concurrently with the ff3DXRD. Here it can be seen that some of the grains experience significant levels of strain and large differences in the maximum and minimum principal strain values with increasing macroscopic load, whilst other grains appear to remain largely unloaded. The loaded grains form a pathway across the sample suggesting force-chain like structures. It can also be noted that, upon unloading, some grains continue to show elevated strain levels indicating grain locking.

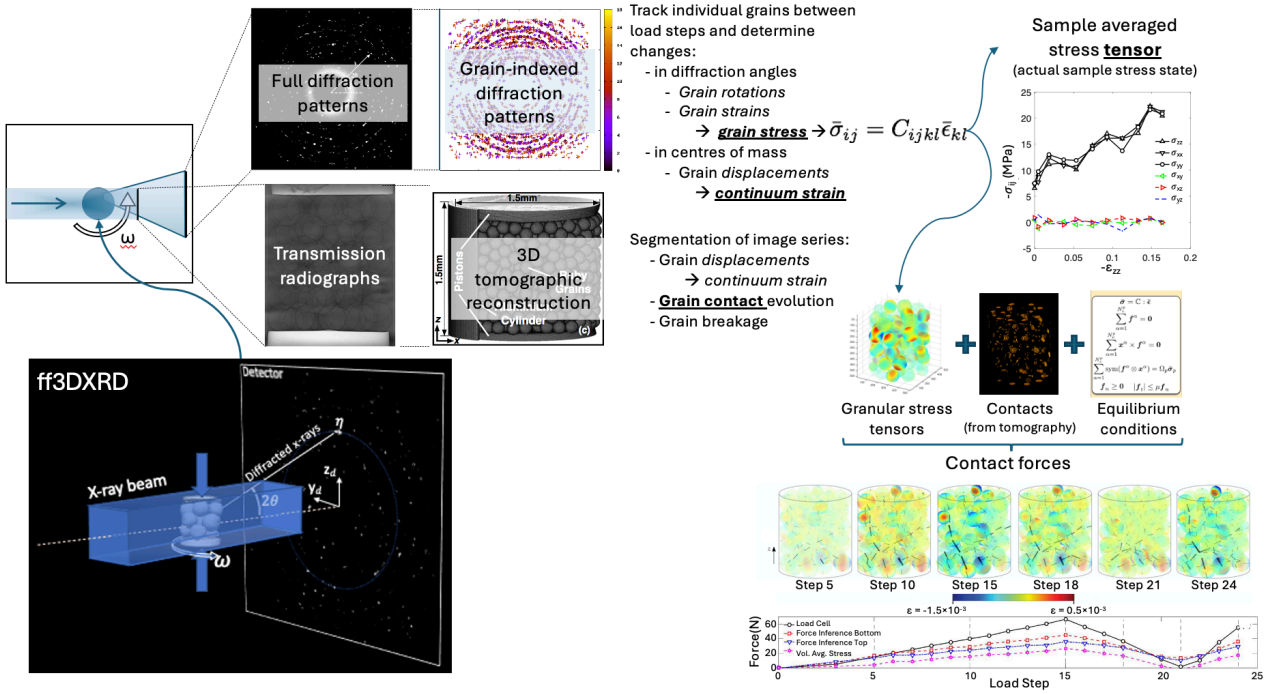

Figure 6. Schematic of the ff3DXRD process for granular mechanics in which a sample is fully illuminated across its diameter by an x-ray beam and either projection (radiography) or diffraction 2D images are acquired during rotation of the samples around the vertical axis. The radiography images provide 3D images of the sample structure. Diffraction peaks corresponding to the individual grains are separated out from the 2D diffraction images and used to determine the crystallographic unit cell parameters for each grain, which provide grain orientation and lattice spacings and their changes across load steps to yield grain rotations and strains. The grain strains, the known anisotropic stiffness tensor, and grain orientation provide the grain-averaged stress tensor, which with contact positions from the tomography images yield the contact forces. (Some images adapted from Hurley et al., 2016).

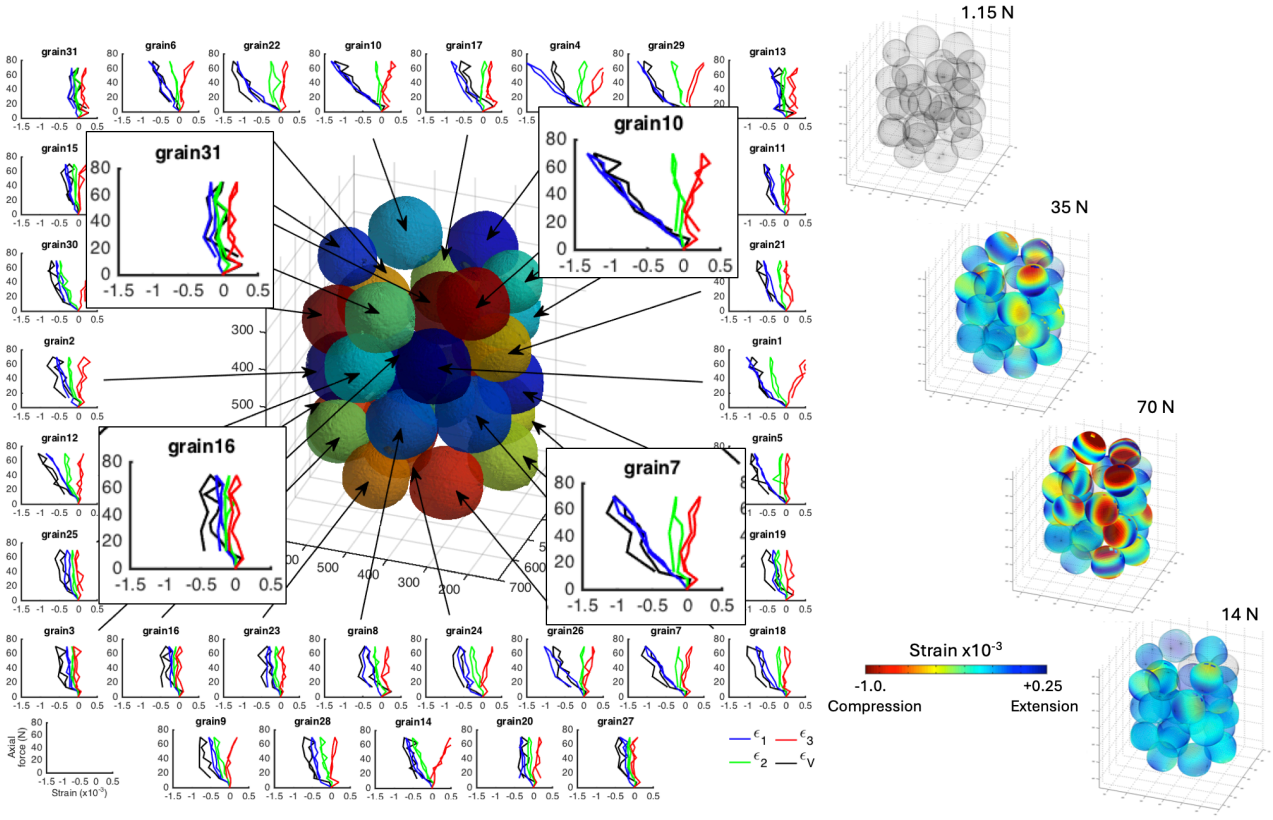

Figure 7. Summary of results from Hall & Wright (2015). Left: Rendering of the grains from the tomography data with colouring representing the individual grain label (X, Y and Z axis dimensions in voxels and the cubic voxels are 2.8 μm wide). Surrounding graphs show the strain tensor data, in terms of the principal and volumetric strains, for each of the grains, plotted against the axial force applied to the sample. The strains are relative to the respective grains' unit cell parameters at the initial load step (1.15 N axial force) and each graph has force (N) on the y-axis and grain strain ($\times 10^{-3}$) on the x-axis. Graphs for four representative grains, either low- or high-loaded, are expanded to show details. Right: 3D renderings of the grain shapes (from the tomography) with the strain ellipsoids rendered onto the surfaces with grain transparency proportional to the volumetric strain and colours indicating the strain magnitude in different directions.

The measured granular strains from 3DXRD are related to the elastic strains in the crystals. Therefore, Hooke's law can be used to determine the per-grain average stress tensors utilising the full anisotropic stiffness tensor and the grain orientations from the 3DXRD. These measurements can then be analysed on a grain-by grain basis, in terms of the assembly behaviour, or averaged to give the sample-averaged 3D stress state. Consequently, ff3DXRD gives access to the full tensorial stress-strain response of the sample. For a large enough sample, this averaging can be applied to sub regions of the sample to investigate local variability in the stress-strain behaviour (e.g., Hurley et al., 2017). Furthermore, Hurley et al. (2016, 2017), developed a methodology based on the 3DXRD-derived granular stresses, granular contacts derived from segmented x-ray tomography images and satisfying equilibrium to infer the contact forces in the imaged granular network, as indicated in Fig. 6. This enables the preferential pathways observed in, e.g., Figure 7, to be characterised as force chains, which was only previously possible through photoelasticity-based (2D) experiments (e.g., Majmudar & Behringer, 2005; Hurley et al., 2014) or with soft particles (e.g., Saadatfar et al., 2012; Brujic et al., 2003; Zhou et al., 2006).

Figures 8 and 9 show representative results from an in-situ triaxial compression experiment on single crystal ruby grains to demonstrate the information that can be derived from the combined ff3DXRD and tomography approach for granular mechanics studies. Figure 8 shows the experimental set-up and tomographic images of the sample evolution plus the force-displacement curve recorded at the sample boundary and the tensor stress-strain response derived from the ff3DXRD measurements. Whilst this experiment was designed to be a standard (albeit small) triaxial compression test, the confining membrane used was rather stiff leading to a more isotropic stress state in the sample, as indicated by the stresses derived from the ff3DXRD; without the 3DXRD data this would not have been detected. Furthermore, the ff3DXRD provides the sample stress tensor data plus tensor strain fields (from the grain displacements) and not just the axial values. These data also show quite a different sample response than that indicated by the boundary measurements,

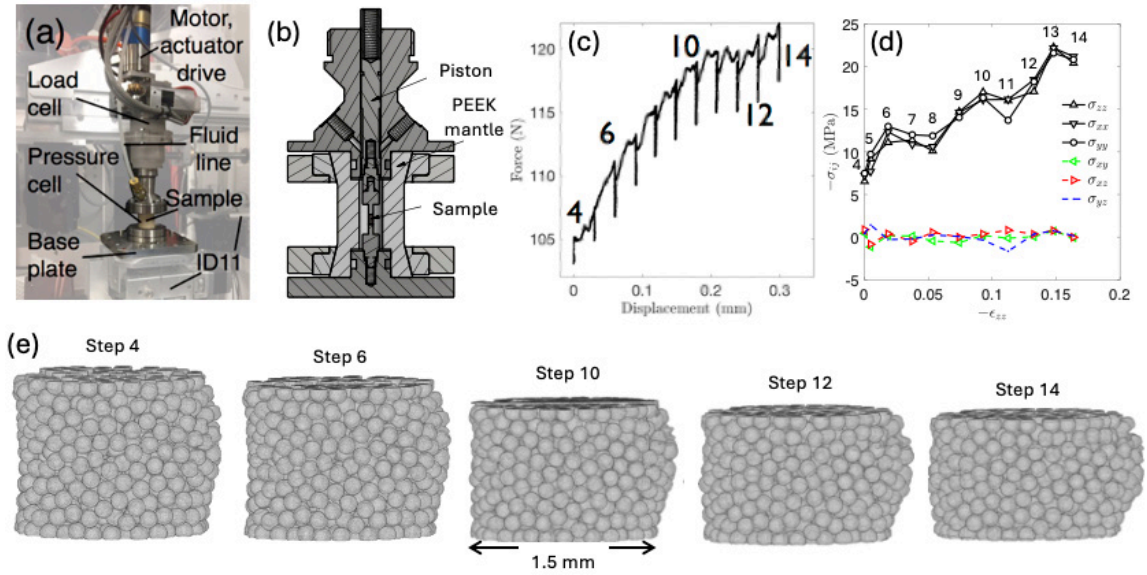

Figure 8. (a) Photograph of the mini triaxial experimental set-up at the ID11 beamline of the ESRF. (b) Cross section of the triaxial device design. The PEEK tube has an internal diameter around the sample of 2.8 mm and the sample diameter was 1.5 mm. (c) Force-displacement curve recorded by the external gauges of the device. (d) Stress-strain curve determined from the volume averaged grain stresses (tensor components) from 3DXRD and the displacements of the grains at the top of the sample versus those at the bottom, respectively. (e) Renderings of the x-ray tomography volumes at selected load steps showing the structural evolution of the sample.

with the latter showing a force plateau that is not really seen in the ff 3DXRD stress-strain data.

The ff3DXRD results in Figure 9 reveal the local details of the sample response in terms of the continuum strain, grain rotations and grain stresses (with just the hydrostatic component of the stress tensor shown) plus the inferred contact force distributions. These figures indicate complex, non-homogeneous sample responses with the development of localised forces/stress in regions of the sample generally offset from regions of higher grain rotations. Further details and discussions can be found in Zhai et al (2019, 2022). The final part of Figure 9 shows 3D contact force histograms from the whole sample at different load steps. These are separated in weak and strong forces and the weaker forces are concentrated more towards the horizontal and stronger forces more towards the vertical (the macroscopic loading axis). Furthermore, evolutions of the contact force distributions can be seen such that, for example, between load step 6 and 8 plus between steps 10 and 12, the dominant orientation of the strong contact forces appears to rotate more towards the vertical and then "release", which coincides with plateaus/slight-reduction in the stress before a stress increase. This indicates the evolution of a "contact force fabric", which is significant in that contact fabric has been cited as being important in defining the mechanical response of granular systems (e.g., Oda, 1972), but the effective fabric will be the force carrying contact network.

Developments and applications of ff3DXRD granular mechanics studies have been presented for artificial quartz, ruby and real sand samples, which can be found in, for example, Alshibli et al. (2013), Cil et al. (2014), Hall & Wright (2015), Hurley et al. (2016), Hurley et al. (2017), Zhai et al. (2019), Imseeh et al. (2020), Shahin et al. (2022), Zhai et al. (2022) and Hurley et al. (2023). Key hurdles to greater exploitation include sample size (which is, in part, limited by the size of the x-ray beam available at synchrotron facilities; most studies have so far been limited to about 1.5 mm diameter samples, limiting the number of grains that can fit in the FoV), as well the number of grains that can be effectively analysed without their diffraction patterns overlapping (which would prevent their separation and individual grain analysis) and the crystal quality of the grains that can be handled (which is also coupled to the number of grains). The latter refers to the fact that the greater the variation in the crystal structure within each individual grain leads to more spread-out diffraction spots, making it harder to separate the diffraction from different grains due to spot overlap as well as meaning spot positions (diffraction angles) are harder to define and track between load steps.

4. Intragranular stress/strain

The ff3DXRD approach described above provides valuable new insights into force transfer and stresses in granular materials under load, including spatial variability and localisation, e.g., force chains. Such spatial variability is not, however, limited to inter-granular variation. The stress, strain and crystal orientation fields within individual grains will also vary due to loading, especially as each grain is loaded by

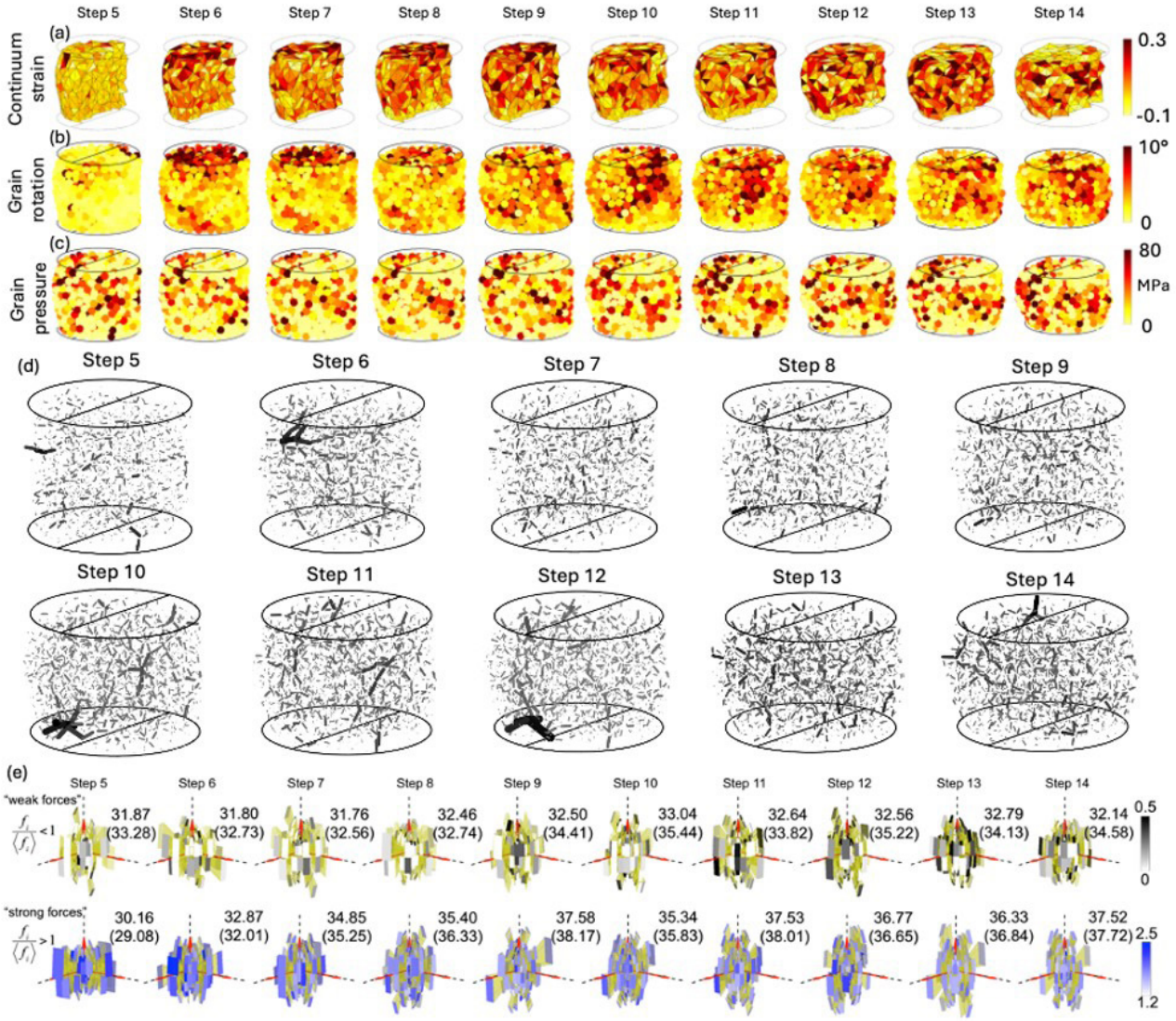

Figure 9. Results from 3DXRD analysis of a system of ruby grains under triaxial compression loading. (a) Incremental continuum strains from triangulated grain centres and their displacements (compression is positive) – the volume cut to reveal the inner structure of the field. (b) Incremental grain (crystallographic axes) rotations. (c) Grain pressures per grain, from the trace of the 3DXRD-derived stress tensor. (d) Inferred contact forces for steps 5-14 (line thickness indicates the contact force magnitude). (e) Spherical histograms of weak and strong contact forces, respectively (excluding boundaries forces) were defined using angular bins directions and the averaged force for each bin is indicated by the colour of the end of each bar. Red arrows indicate x-axis, y-axis and z-axis with lengths corresponding to force distribution probabilities of 0.02, 0.02, 0.005, respectively. The numbers indicate the average inclination of the contacts and force-weighted contact orientations (in parentheses). C. Zhai is acknowledged for producing the images.

multiple contacts. Furthermore, natural variations in the crystal parameters with or without applied loads, are likely in natural sand grains. To investigate the internal granular structure and stress/strain fields requires an alternative approach that can yield the fields of these properties within each grain. This can be achieved by scanning a sample across a small x-ray beam by vertical and horizontal translations (in Δy and Δz in Figure 10) such that each recorded 2D diffraction pattern represents the diffraction along a line integral defined by the intersection of the beam and the sample. If at each Δy position for each Δz height the sample is rotated over 180°, tomographic principles can be used to reconstruct the unit cell parameters for each voxel within a single Δz slice; this can be referred to as scanning-3DXRD (s3DXRD) (Henningsson et al., 2020; Henningsson, 2023). Repeating this procedure over a range of Δz positions allows a full 3D volume to be defined in which each voxel contains the crystallographic parameters for that point in the grain assembly. Simplifications of the calculations allow the crystallographic strain to be more easily determined, but the full unit cell parameters can also be defined on a per-voxel basis (Henningsson et al., 2020; Henningsson, 2023). As with the strains from ff3DXRD, the voxel strains from s3DXRD can be

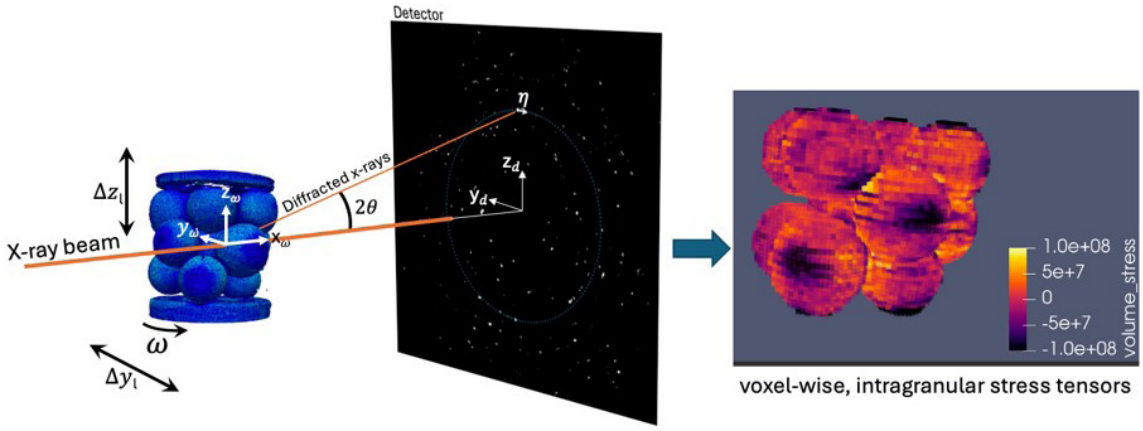

Figure 10. Left: schematic of the s3DXRD experimental approach where the sample is scanned through a small x-ray beam over a range of Δy positions with 180° sample rotation at each position to record a series of 2D x-ray diffraction images that can be treated to yield voxel-wise tensorial measures of the crystallographic strain/stress. Right: example of a s3DXRD-derived 3D stress field (volumetric component of the stress tensors shown) for an assembly of 12 single crystal quartz-grains loaded under confined 1D compression (upper and lower pistons and the side walls; not shown in rendering) (Vestin, 2022). The sample width is about 1.4 mm and the grains are about 300 μm in diameter.

interpreted in terms of the local stress tensor through Hooke's law and the 3D stiffness tensor of the grain material rotated to the local crystallographic orientation. Figure 10 outlines the experimental measurement set-up for an experiment at ID11 at the ESRF and an example of the output from the s3DXRD in the form of the volumetric components of the voxel-wise defined stress tensors in an assembly of single-crystal quartz grains loaded in confined uniaxial compression. The rendering indicates regions of compression in the grains where they contact with the boundaries and at the granular contacts, as well as dilating regions between the contacts.

The potential for the s3DXRD approach for improved understanding of granular systems is significant in terms of gaining access to the intra-granular stress fields and how, for example, these evolve towards eventual grain failure and for a more detailed understanding of contact mechanisms (particularly if combined with high-resolution tomography imaging), all in the context of a multi-grain 3D system. Further results will be presented in upcoming papers.

5. Imaging of granular dynamics

The preceding examples have demonstrated the increasing detail that it is possible to achieve through advanced 3D x-ray measurement techniques, but are all limited to quasi-static experiments. X-ray tomography can now be run for small samples at synchrotron facilities with time resolutions in the order of a second (the resolution is defined by how long it takes to acquire the data to generate the 3D image). This means that continuous loading experiments can be run if the loading rate is slow enough to provide less than about half a voxel width displacement during a scan. However, many processes in granular mechanics are more dynamic and 1 tomography/s is too slow to capture such phenomena and faster tomographic imaging requires fast rotations (e.g., García-Moreno et al., 2019), which can influence the sample response. An alternative is to limit the imaging to 2D, which has previously been done with high-speed photography of a sample surface (e.g., Borg et al., 2013), but viewing the sample surface leaves uncertainties about what is happening in the bulk of the sample versus surface interaction effects. High-speed x-ray radiography provides the possibility to follow sample evolution also in the bulk of a sample, albeit in 2D and with averaging through the sample thickness (e.g., for granular materials, Royer et al., 2005, 2007; Gupta et al., 2021; Méjean et al., 2022; Thakur et al., 2024).

Figure 11 shows an example of high-speed x-ray radiography (100 000 frames/s) of a gravity-driven impact of a steel ball into a dry granular bed (glass beads) acquired at the ID19 beamline of the ESRF. The top row of images shows a series of radiography images of the impact 10 frames (0.1 ms) apart in time. From these images, the impact of the ball and the resulting cratering and ejector can be observed. The full radiographic sequence provides a 3D volume defined by the horizontal (x) and vertical (y) axes plus the time (t) axis. This volume can be sliced along the time axis to give a (t,y) image in which gradients indicate the vertical velocity of the different components of the system (Figure 11, middle row). Consequently, the trajectory and, thus, the velocity of the impacting ball and its deceleration can be determined from the (t,y) gradient (as indicated in the lower image). This (t,y) image can be enhanced by, for the whole time-sequence, subtracting the preceding image to provide an incremental difference image (i.e., $I_{diff}(t) = I(t)-I_{(t-1)}$), which highlights changes in the image between time frames. The bottom row of Figure 11 shows such an I_{diff} image and the propagation of a shockwave through the granular bed from the impact point can be clearly seen and its velocity measured from the

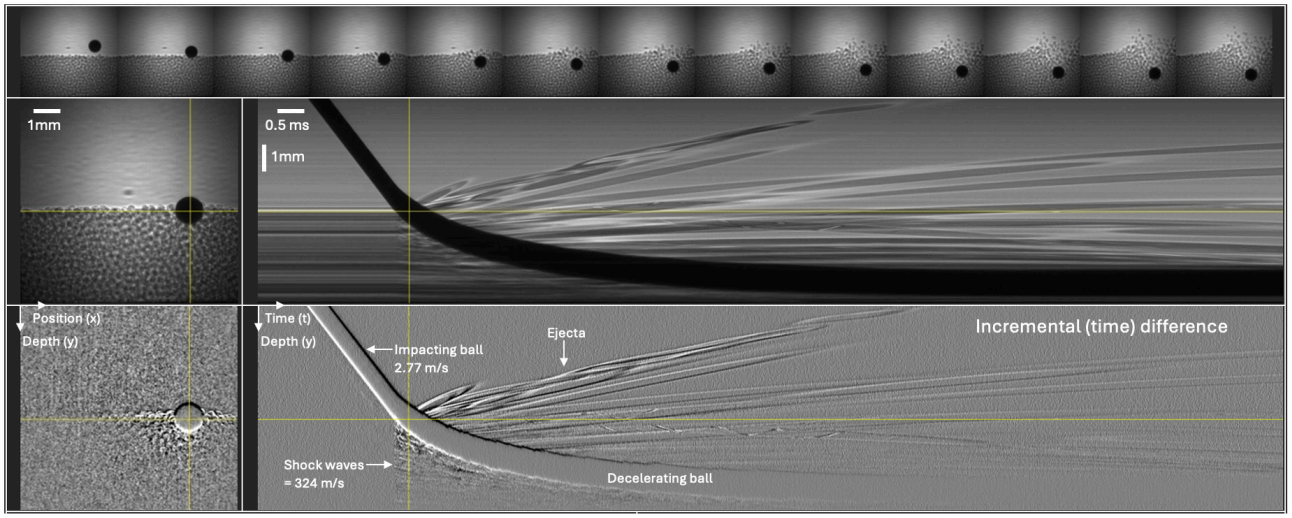

Figure 11. Fast x-ray radiography of the impact of a 3 mm diameter iron ball traveling at about 2.77 m/s into a bed of 0.3 mm diameter glass beads (100 kHz image acquisition, 8.39 μs shutter speed and 20 μm pixel size). Top: snapshots from image sequence over 1.2 ms (every 10th image shown – interval 0.1ms). Middle: x-y (radiography) image for a single time frame and *y*-*t* slice from the 3D (*x,y,t*) volume. Bottom: the same slices extracted from the incremental difference $I_{diff}(x,y,t)$ volume. The initial propagating wave (about 324 m/s) can be seen below the first point of impact. Images acquired at ID19 at the ESRF.

gradient. The shockwave velocity is estimated to be about 324 m/s, although it is noted that the time resolution possible with the 100 kHz imaging plus the given pixel size and FoV, limit this quantification.

The described high-speed radiography measurements have the potential to reveal new details towards understanding dynamic processes such as impacts into granular beds, but the limitation to 2D will always require adapted experiments and appropriate interpretation considering the 2D boundary conditions, even if some 3D information can be derived from dynamic 2D imaging and associated static 3D images (e.g., Gupta et al., 2021; Kuwik et al., 2024). The possibility to perform high-speed 3D x-ray imaging of dynamic processes without sample rotation is currently a key topic of research, but requires further development of both acquisition methodologies and data analysis approaches (e.g., Henningsson & Hall, 2021; Villanueva-Perez, et al., 2023, Asimakopoulou et al., 2024).

6. Summary and conclusion

This paper has provided an overview of some experimental developments and results from the last 15-20 years that have provided new opportunities for enhanced experimental description of deformation processes in granular materials. This overview has described, primarily, work of the author with different collaborators and is not a comprehensive view of the field but aims to give a snapshot of some of the new possibilities in experimental granular mechanics. The described experimental approaches exploit x-ray imaging and 3D x-ray diffraction to describe granular structures and their evolution under different mechanical loads at the granular assembly, inter-granular and intra-granular scales, including continuum strains and granular strains/stresses. The different methods provide access to different structural scales and their use in combination can provide important multi-scale insight. Continuing developments are pushing the limits in terms of temporal and spatial resolutions, as well as possible FoVs, which are all essential to enable experiments of increasing relevance in terms of granular systems with reduced boundary influences. The consequence of the increased resolution and FoV size is the increase in data volumes, which will require even more efficient data analysis algorithms, but will also offer great possibilities for our understanding of evolving granular systems.

Acknowledgements

The work described in this paper is a summary of a number of projects over the past 20 years involving many collaborators. In particular, E. Andò, G. Viggiani, N. Lenoir and J. Desrues (Laboratoire 3SR, Grenoble) contributed greatly to the developments described concerning the 4D x-ray microtomography imaging of in-situ triaxial compression tests on sand (and continue to make important advances in this area). Parts of Figure 2 were originally created by E. Andò. The 3DXRD developments would not have been possible without the support and expertise of J. Wright (ID11, ESRF). The described ESRF beamtimes for 3DXRD at ID11 were also supported by M. Majkut and W. Ludwig (ESRF). R. Hurley (John Hopkins University) was key to the developments in force transfer analysis from the 3DXRD experiments and has since driven forward the use

of 3DXRD in geomechanics, as described, for example, in the cited references. C. Zhai (John Hopkins University) is acknowledged for providing the images in Figure 9. The dynamic x-ray imaging experiment at ID19 was run by J. Åhlund (Scandiflash) with E. Larsson (Lund University) and supported by B. Lukic and A. Rack (ID19, ESRF). A. Henningsson (Lund University) has driven the development of s3DXRD and the results shown were produced by P. Vestin (Lund University), both under supervision of the author. J. Engqvist (Lund University) was key to the development of many of the described experimental set-ups. The described ESRF experiments were performed under granted beamtimes, ma280, ma828, ma1216, ma1913, ma2665, ma3373, ma4200, ma4493 and in1126. Some of the work was performed within the framework of funding from Vetenskapsrådet projects (#2012-04234 and #2015-04398).

Declaration of interest

The author has no conflicts of interest to declare.

Data availability

The raw data from the ESRF experiments in this paper are available through the ESRF data portal.

List of symbols and abbreviations

2D	two dimensional
2θ	diffraction angle in Bragg's law multiplied by 2,
3D	three dimensional
3DXRD	three-dimensional X-ray Diffraction
4D	four dimensional
d_{hkl}	crystallographic plane spacing for planes defined by the Miller indices h, k, l
dx, dy, dz	displacements in x,y and z directions from DVC
h, k, l	Miller indices describing different planes in a crystal lattice
q	deviatoric stress in triaxial compression testing
s3DXRD	scanning Three-dimensional X-ray Diffraction
x, y, t	2D spatial axes (x,y) plus time axis (t)
DVC	digital Volume Correlation
D-DVC	discrete Digital Volume Correlation
ESRF	European Synchrotron Radiation Facility
FoV	Field of View
Ff3DXRD	Full-field Three-dimensional X-ray Diffraction
I_{diff}	difference image derived from ($I_t - I_{t-1}$)
I_t	image at time *t*
I_{t-1}	image at time *t-1*
SPAM	Software for Practical Analysis of Materials
Δy, Δz	motor translations used in scanning 3DXRD (y – horizontal, z – vertical)
λ	x-ray wavelength,

References

Alshibli, K., Cil, M.B., Kenesei, P., & Lienert, U. (2013). Strain tensor determination of compressed individual silica sand particles using high-energy synchrotron diffraction. *Granular Matter*, 15, 517-530

Andò, E. (2013). *Experimental investigation of microstructural changes in deforming granular media using x-ray tomography* [Doctoral thesis, Université de Grenoble]. Université de Grenoble.

Andò, E., Hall, S.A., Viggiani, G., Desrues, J., & Bésuelle, P. (2012). Experimental micromechanics: grain-scale observation of sand Deformation. *Géotechnique Letters*, 2, 107-112.

Andò, E., Viggiani, G., Hall, S.A., & Desrues, J. (2013). Experimental micro-mechanics of granular media studied by x-ray tomography: recent results and challenges. *Géotechnique Letters*, 3, 142-146.

Arthur, J.R.F., & Dunstan, T. (1969). Radiography measurements of particle packing. *Nature*, 223, 464-468.

Asimakopoulou, E.M., Bellucci, V., Birnsteinova, S., Yao, Z., Zhang, Y., Petrov, I., Deiter, C., Mazzolari, A., Romagnoni, M., Korytar, D., Zaprazny, Z., Kuglerova, Z., Juha, L., Lukić, B., Rack, A., Samoylova, L., Garcia-Moreno, F., Hall, S.A., Neu, T., Liang, X., Vagovic, P., & Villanueva-Perez, P. (2024). Development towards high-resolution kHz-speed rotation-free volumetric imaging. *Optics Express*, 32, 4413-4426.

Borg, J.P., Morrissey, M.P., Perich, C.A., Vogler, T.J., & Chhabildas, L.C. (2013). In situ velocity and stress characterization of a projectile penetrating a sand target: experimental measurements and continuum simulations. *International Journal of Impact Engineering*, 51, 23-35.

Brujic, J., Edwards, S.F., Grinev, D.V., Hopkinson, I., Brujic, D., & Makse, H.A. (2003). 3D bulk measurements of the force distribution in a compressed emulsion system. *Faraday Discussions*, 123, 207-220.

Cil, M.B., Alshibli, K., Kenesei, P. & Lienert, U. (2014). Combined high-energy synchrotron X-ray diffraction and computed tomography to characterize constitutive behavior of silica sand. *Nucl. Instrum. Methods Phys. Res. B: Beam Interact Mater At*, 324, 11-16

Desrues, J., Andò, E., Mevoli, F.A., Debove, L., & Viggiani, G. (2018). How does strain localise in standard triaxial tests on sand: revisiting the mechanism 20 years on. *Mechanics Research Communications*, 92, 142-146.

Desrues, J., Chambon, R., Mokni, M., & Mazerolle, F. (1996). Void ratio evolution inside shear bands in triaxial sand specimens studied by computed tomography. *Geotechnique*, 46, 529-546.

García-Moreno, F., Kamm, P.H., Neu, T.R., Bülk, F., Mokso, R., Schlepütz, C.M., Stampanoni, M., & Banhart, J. (2019). Using X-ray tomoscopy to explore the dynamics of foaming metal. *Nature Communications*, 10, 3762.

Gupta, A., Crum, R.S., Zhai, C., Ramesh, K.T., & Hurley, R.C. (2021). Quantifying particle-scale 3D granular dynamics during rapid compaction from time-resolved in situ 2D x-ray images. *Journal of Applied Physics*, 129(22)

Hall, S.A. (2012). Digital image correlation in experimental geomechanics. In G. Viggiani, S.A. Hall & E. Romero (Eds.), *ALERT Doctoral School 2012: Advanced experimental techniques in geomechanics:* (pp. 69-102). ALERT Geomaterials.

Hall, S.A., & Wright, J. (2015). Three-dimensional experimental granular mechanics. *Géotechnique Letters*, 5, 236-242.

Hall, S.A., Bornert, M., Desrues, J., Pannier, Y., Lenoir, N., Viggiani, G., & Bésuelle, P. (2010a). Discrete and Continuum analysis of localised deformation in sand using X-ray micro CT and Volumetric Digital Image Correlation. *Geotechnique*, 60, 315-322.

Hall, S.A., Lenoir, N., Viggiani, G., Bésuelle, P., & Desrues, J. (2010b). Characterisation of the evolving grain-scale structure in a sand deforming under triaxial compression. In K.A. Alshibli & A.H. Reed (Eds.), *Advances in computed tomography for geomaterials, GeoX 2010* (p. 34-42). Wiley & Sons.

Hall, S.A., Desrues, J., Viggiani, G., Bésuelle, P., & Andò, E. (2012). Experimental characterisation of (localised) deformation phenomena in granular geomaterials from sample down to inter- and intra-grain scales, in Full field measurements and identification in Solid Mechanics. *Procedia IUTAM*, 4, 54-65.

Hall, S.A., Wright, J., Pirling, T., Andò, E., Hughes, D.J., & Viggiani, G. (2011). Can intergranular force transmission be identified in sand? First results of spatially-resolved neutron and x-ray diffraction. *Granular Matter*, 13, 251-254.

Henningsson, A. (2023). *Inferring crystal strain distributions from X-ray diffraction data: analytical and computational advances* [Master's dissertation]. Division of Solid Mechanics, Lund University.

Henningsson, A., & Hall, S.A. (2021). A continuity flow based tomographic reconstruction algorithm for 4d multi-beam high temporal: low angular sampling. *Journal of Imaging*, 7, 246.

Henningsson, N.A., Hall, S.A., Wright, J.P., & Hektor, J. (2020). Reconstructing intragranular strain fields in polycrystalline materials from scanning 3DXRD data. *Journal of Applied Crystallography*, 53, 314-325.

Hurley, R., Marteau, E., Ravichandran, G., & Andrade, J.E. (2014). Extracting inter-particle forces in opaque granular materials: beyond photoelasticity. *Journal of the Mechanics and Physics of Solids*, 63, 154-166.

Hurley, R.C., Hall, S.A., & Wright, J. (2017). Multi-scale mechanics of granular solids from grain-resolved X-ray measurements. *Proc. R. Soc. A*, 473, 20170491.

Hurley, R.C., Hall, S.A., Andrade, J.E., & Wright, J. (2016). Quantifying Interparticle Forces and Heterogeneity in 3D Granular Materials. *Physical Review Letters*, 117, 098005.

Hurley, R.C., Shahin, G., Kuwik, B.S., & Lee, K. (2023). Assessing continuum plasticity postulates with grain stress and local strain measurements in triaxially compressed sand. *Proceedings of the National Academy of Sciences of the United States of America*, 120, e2301607120.

Imseeh, W.A., Alshibli, K.A., Moslehy, A., Kenesei, P., & Sharma, H. (2020). Influence of crystal structure on constitutive anisotropy of silica sand at particle-scale. *Computers and Geotechnics*, 126, 103718.

Jaeger, H.M., Nagel, S.R., & Behringer, R.P. (1996). Granular solids, liquids, and gases. *Reviews of Modern Physics*, 68, 1259.

Kuwik, B.S., Moreno, J., Shaeffer, M., Simpson, G., & Hurley, R.C. (2024). The response of dry and wet silica sand to high velocity impact. *International Journal of Impact Engineering*, 186, 104883.

Majmudar, T.S., & Behringer, R.P. (2005). Contact force measurements and stress induced anisotropy in granular materials. *Nature*, 435, 1079-1082.

Méjean, S., Guillard, F., Faug, T., & Einav, I. (2022). X-ray study of fast and slow granular flows with transition jump in between. *Granular Matter*, 24, 26.

Oda, M. (1972). The Mechanism of Fabric Changes During Compressional Deformation of Sand. *Soil and Foundation*, 12, 1-18.

Pinzón, G., Andò, E., Desrues, J., & Viggiani, G. (2023). Fabric evolution and strain localisation in inherently anisotropic specimens of anisometric particles (lentils) under triaxial compression. *Granular Matter*, 25, 15.

Poulsen, H.F. (2008). *Three-Dimensional X-Ray diffraction microscopy: mapping polycrystals and their dynamic*s. Springer.

Royer, J.R., Corwin, E.I., Eng, P.J., & Jaeger, H.M. (2007). Gas-mediated impact dynamics in fine-grained granular materials. *Physical Review Letters*, 99, 038003.

Royer, J.R., Corwin, E.I., Flior, A., Cordero, M.-L., Rivers, M.L., & Eng, P.J. (2005). Formation of granular jets observed by high-speed X-ray radiography. *Nature Physics*, 1, 164-167.

Saadatfar, M., Sheppard, A.P., Senden, T.J., & Kabla, A.J. (2012). Mapping forces in a 3D elastic assembly of grains. *Journal of the Mechanics and Physics of Solids*, 60, 55-66.

Shahin, G., Herbold, E.B., Hall, S.A., & Hurley, R.C. (2022). Quantifying the hierarchy of structural and mechanical length scales in granular systems. *Extreme Mechanics Letters*, 51, 101590.

Stamati, O., Andò, E., Roubin, E., Cailletaud, R., Wiebicke, M., Pinzon, G., Couture, C., Hurley, R.C., Caulk, R., Caillerie, D., Matsushima, T., Bésuelle, P., Bertoni, F., Arnaud, T., Ortega Laborin, A., Rorato, R., Sun, Y., Tengattini, A., Okubadejo, O., Colliat, J.-B., Saadatfar, M., Garcia, F.E., Papazoglou, C., Vego, I., Brisard, S., Dijkstra, J., & Birmpilis, G. (2020). Spam: software for practical analysis of materials. *Journal of Open Source Software*, 5, 2286.

Stone, K.J.L. (1985). *Shear band formation in granular materials* [Doctoral thesis]. Cambridge University.

Thakur, M.M., Ghosh, S., & Hurley, R.C. (2024). On rapid compaction of granular materials: combining experiments with in-situ imaging and mesoscale modeling. *Journal of the Mechanics and Physics of Solids*, 186, 105576.

Vestin, P. (2022). *Estimation and interpretation of the intra-granular stress and strain evolution in a uniaxially loaded silica sample using scanning x-ray diffraction* [Master's dissertation]. Division of Solid Mechanics, Lund University.

Viggiani, G., & Hall, S.A. (2012). Full-field measurements in experimental geomechanics: historical perspective, current trends and recent results. In G. Viggiani, S.A. Hall & E. Romero (Eds.), *ALERT Doctoral School 2012: Advanced experimental techniques in geomechanics* (pp. 3-68). ALERT Geomaterials.

Villanueva-Perez, P., Bellucci, V., Zhang, Y., Birnsteinova, S., Graceffa, R., Adriano, L., Myrto Asimakopoulou, E., Petrov, I., Yao, Z., Romagnoni, M., Mazzolari, A., Letrun, R., Kim, C., Koliyadu, J.C.P., Deiter, C., Bean, R., Giovanetti, G., Gelisio, L., Ritschel, T., Mancuso, A., Chapman, H.N., Meents, A., Sato, T., & Vagovic, P. (2023). Megahertz X-ray Multi-projection imaging, arXiv:2305.11920.

Wiebicke, M., Andò, E., Viggiani, G., & Herle, I. (2020). Measuring the evolution of contact fabric in shear bands with X-ray tomography. *Acta Geotechnica*, 15, 79-93.

Wright, J. (2020). *ImageD11 (python code for identifying individual grains in spotty area detector X-ray diffraction images)*. Retrieved in May 30, 2024, from https://github.com/FABLE-3DXRD/ImageD11

Zhai, C., Albayrak, N., Engqvist, J., Hall, S.A., Herbold, E.B., & Hurley, R.C. (2022). Quantifying local rearrangements in 3D granular materials: rearrangement measures, correlations, and relationship to stresses. *Physical Review. E*, 105, 014904.

Zhai, C., Herbold, E.B., Hall, S.A., & Hurley, R.C. (2019). Particle rotations and energy dissipation during mechanical compression of granular materials. *Journal of the Mechanics and Physics of Solids*, 129, 19-38.

Zhao, C.F., Pinzón, G., Wiebicke, M., Andò, E., Kruyt, N.P., & Viggiani, G. (2021). Evolution of fabric anisotropy of granular soils: x-ray tomography measurements and theoretical modelling. *Computers and Geotechnics*, 133, 104046.

Zhou, J., Long, S., Wang, Q., & Dinsmore, A.D. (2006). Measurement of forces inside a three-dimensional pile of frictionless droplets. *Science*, 312, 1631-1633.